Three-dimensional woodpile photonic crystal templates for the infrared spectral range

Vygantas Mizeikis, Kock Khuen Seet, Saulius Juodkazis, and Hiroaki Misawa

Core Research for Evolutionary Science and Technology, Japan Science and Technology Corporation, Research Institute for Electronic Science, Hokkaido University, Sapporo 060-0812, Japan

Received March 29, 2004

High-quality templates of three-dimensional woodpile photonic crystals are fabricated in photoresist SU-8 by use of femtosecond laser lithography. The samples have smooth surfaces, are mechanically stable, and are resistant to degradation under environmental and chemical influences. Fundamental and higher-order photonic stopgaps are identified in the wavelength range 2.0–8.0 μm. These templates can be used for subsequent infiltration by optically active or high-refractive-index materials. © 2004 Optical Society of America

OCIS codes: 220.4000, 220.4610, 230.4000, 160.5470.

Photonic crystals[1] (PhCs) are periodic dielectric structures that are expected to play an important role in optics and optoelectronics due to their unique capabilities in controlling the emission and propagation of light by means of photonic bandgap (PBG) effects.[2] These capabilities can be best exploited in three-dimensional (3D) PhCs. Since direct, large-scale 3D microfabrication of PhCs from semiconductors has proved to be tedious,[3,4] cheaper and simpler fabrication strategies are in high demand. Some of these strategies involve microfabrication of so-called PhC templates with more-feasible techniques and materials. The templates can be subsequently infiltrated by other materials with higher refractive indices. For example, opal templates, obtained by self-organized sedimentation of microspheres from colloidal suspensions,[5,6] have been infiltrated by Si, InP, and other materials.[7,8] However, this technique is limited to opallike structures only, and it does not allow the easy inclusion of nonperiodic defects, which are indispensable for controlling electromagnetic radiation in PhCs.

Laser lithography is a microstructuring technique based on drawing using the focal spot of a focused laser beam in the bulk of dielectric materials.[9,10] High power density, achieved by focusing and ultrashort pulse excitation, allows multiphoton absorption to be induced inside regions smaller than the diffraction-limited focal spot size. Multiphoton absorption can trigger permanent photomodification, thus permitting the drawing of nearly arbitrarily shaped structures by translation of the focal spot. Such flexibility makes 3D laser lithography a versatile tool for the fabrication of PhC templates.[11] So far, the most successful results have been achieved in liquid resins in which microstructures were generated through photosolidification.[9,12,13] However, resin-based structures often degrade structurally after fabrication as a result of shrinkage and their general susceptibility to various environmental factors.[14] In this respect epoxy-based negative photoresist SU-8 seems to be an attractive alternative. Periodic structures have already been fabricated in SU-8 by use of the interference of multiple laser beams.[15] However, since this method is poorly suited for defect engineering, 3D lithographic drawing would allow one to obtain structures with much broader functionality. Here we report the use of the latter technique for the fabrication of 3D PhC structures in SU-8. The samples obtained have good quality, exhibit signatures of photonic stopgaps at infrared wavelengths, and can be easily tailored to include structural defects.

The setup for 3D laser lithography used the pulsed output of a Hurricane X system (Spectra-Physics) with $\tau_{\mathrm{pulse}} = 120$ fs and $\lambda_{\mathrm{pulse}} = 800$ nm as the light source. The fabrication was performed in an optical microscope (Olympus IX71) equipped with oil-immersion objective lenses (magnification of 60× and 100×, with a N.A. of 1.4 and 1.35, respectively). The 3D drawing was accomplished by mounting the samples on a piezoelectric-transducer-controlled 3D translation stage (Physik Instrumente PZ48E), which has a maximum positioning range of up to 50 μm and accuracy of several nanometers. The samples were films of SU-8 (Microchem)[16] formulation 50, spin coated to a 50-μm thickness on glass substrates. Single-photon absorption in SU-8 is negligible at λ_{pulse} but becomes dominant at $\lambda = 400$ nm.[16] Therefore two-photon absorption is responsible for the photomodification by the cross linking of a polymer, which renders SU-8 stable against subsequent chemical development. The development removes unexposed SU-8, leaving only solid exposed parts that have a refractive index of $n \approx 1.6$ at infrared wavelengths when suspended in air ($n = 1$).

For the experiments a woodpile structure, shown in Fig. 1(a), was chosen. The woodpile structure is widely popular because of its diamondlike character, pronounced PBG properties, and the possibility of layer-by-layer fabrication.[17] Figures 1(b) and 1(c) show scanning electron microscopy (SEM) images of the woodpile sample recorded in SU-8. The recording was done by translation of the sample in small $\Delta l = 80$ nm steps along the rod lines with single-pulse exposure on each step. The low pulse energies used ($I = 0.55$ nJ) confirm that an unamplified Ti:sapphire laser is sufficient for the fabrication of SU-8.[18]

0146-9592/04/172061-03$15.00/0

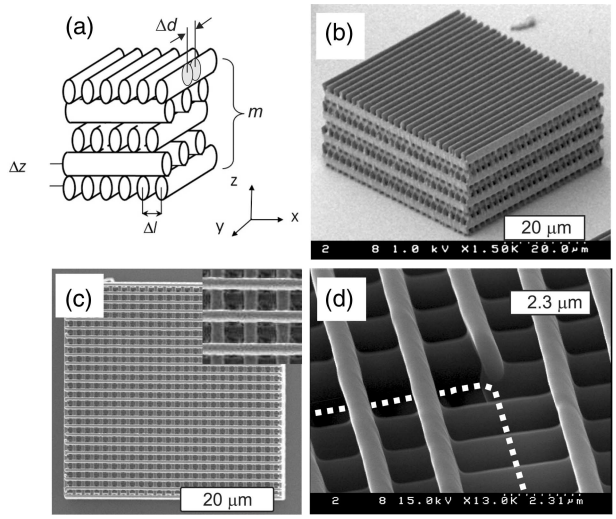

Fig. 1. (a) Woodpile geometry and its main parameters: Δl, distance between the rods; Δz, distance between the layers; m, number of layers; Δd, focal spot scan step. Note that the rods have elliptical cross-sectional shapes. (b), (c) SEM images of the woodpile PhC template with parameters $\Delta l = 2.0\ \mu$m, $\Delta z = 1.4\ \mu$m, and $m = 14$ recorded by translation of the sample in steps of $\Delta d = 0.08\ \mu$m with $I = 0.55$ nJ pulses focused by a 60×, 1.4-N.A. objective. (d) Demonstration of linear defect with a 90° bend; the tentative light flow direction is indicated by the dotted curve. For easier visualization the defect is formed at the top of the structure.

The SEM images in Figs. 1(b) and 1(c) demonstrate that the sample is a perfect parallelepiped with dimensions of 48 μm × 48 μm × 21 μm. Its size in the $x-y$ plane is limited only by the range of the translation stage, whereas along the z axis it is limited to approximately 40 μm by the requirement to maintain uniform, aberration-free focusing. The structures retain their shape even after being dislodged from the substrates and have not degraded within at least several months after fabrication. The individual rods have smooth surfaces and elliptical cross sections with diameters of 0.5 μm ($x-y$ plane) and 1.3 μm (z axis) adjustable within a certain range by changing the pulse energy. Elongation in the focusing direction by a factor of approximately 2.6 is due to the ellipsoidal shape of the focal region and forces an increase in the distance Δz to avoid an unacceptably high overlap between the neighboring layers tantamount to monolithic SU-8. For the sample shown in Figs. 1(b) and 1(c), $\Delta z/\delta l = 1/\sqrt{2}$, which corresponds to stretching of a face-centered-cubic unit cell by a factor of 2.

Figure 1(c) demonstrates the possibilities of the defect engineering. The missing halves of two rods in the two neighboring top layers are connected to form a waveguide with a 90° bending angle as proposed in the literature.[4,19] Although the refractive index of SU-8 is too low to achieve real waveguiding, this example illustrates that defects with the required geometry can be easily created by simply shutting off the laser beam for appropriate time intervals during the recording. This would be impossible to achieve by recording with multiple beam interference fields, which can generate periodic patterns only.

Figure 2 shows the reflection spectrum of the sample shown in Figs. 1(b) and 1(c) measured along the z axis by a Fourier transform infrared spectrometer (Valor III, Jasco) with a microscope attachment (Micro 20, Jasco). Two major high-reflectance regions can be seen centered at $\lambda = 7.0$ and 3.6 μm, along with two weaker peaks centered at 2.6 and 2.1 μm. Their shapes and relative amplitudes are well reproduced by the theoretical spectrum obtained by the transfer-matrix calculations,[20] shown in the same figure. The model structures consisted of elliptical rods with $n = 1.6$; major and minor axes of 1.3 and 0.5 μm, respectively; and other parameters (Δl, Δz, m) matching those of the sample. At shorter wavelengths of $\lambda = 1.6-2.8\ \mu$m, both experiment and calculations yield two reflectivity peaks, but their spectral positions and amplitudes do not match. These differences are most likely due to unaccounted experimental factors, such as disorder, spread of the incidence angles, and others. Nevertheless, the two spectra are qualitatively similar, even at shorter wavelengths.

Figure 3 shows the measured reflectivities of three other structures with lattice parameters scaled down compared with the previous sample. The spectral positions of the major reflectivity peaks in these samples depend on the lattice scaling factor in agreement with Maxwell's scaling behavior[21] (see inset), which constitutes clear evidence of their photonic band nature. Observation of multiple reflectivity peaks can be explained by the presence of multiple stopgaps or forbidden spectral ranges existing along certain directions only. Higher-order stopgaps are evidence that good structural quality was achieved, because higher photonic bands are more susceptible to disorder. In addition, they can be exploited to achieve PBG effects in structures with larger structural parameters.[22] The shortest wavelength of a reliably detected stopband, 2.11 μm, is already fairly

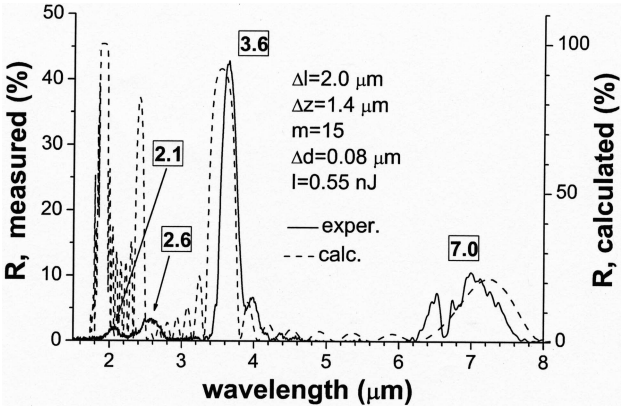

Fig. 2. Infrared reflectivity spectrum of the sample shown in Figs. 1(a) and 1(b) (solid curve) and the same spectrum calculated using the transfer-matrix technique (dashed curve). The small dip at $\lambda = 6.6\ \mu$m in the experimental spectrum is due to the intrinsic absorption of SU-8. The center wavelengths of various peaks are indicated by numbers.

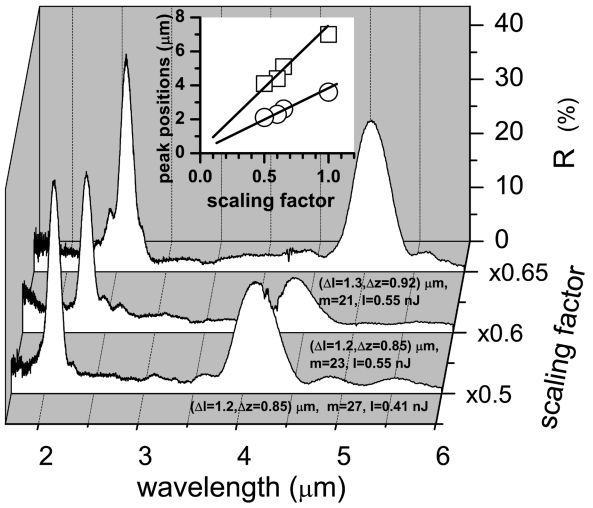

Fig. 3. Reflectivity spectra of three samples with lattice parameters scaled down with respect to the sample shown in Fig. 2. Inset, positions of the reflectivity peaks versus the lattice scaling factor plotted for all four samples. The solid lines are guides to the eye to emphasize the linear scaling.

close to the optical communications spectral region (1.1–1.6 μm). In the future it may become possible to reach this spectral region by further scaling down the parameters of the woodpile structure. This can be achieved by reducing the laser wavelength and by using photoresists with single-photon absorption onset at shorter wavelengths.

In conclusion, 3D woodpile structures were fabricated in SU-8 by means of femtosecond laser lithography. The flexibility of the fabrication method allowed large-scale samples to be obtained and allowed defects to be easily introduced into them. The use of a commercially available photoresist SU-8 allowed structures to be obtained that are mechanically stable and can withstand a wide range of thermal and chemical influences. The structures were found to exhibit pronounced signatures of fundamental and higher-order photonic stopgaps in the infrared wavelength range 2.0–8.0 μm. Although the fabricated samples were not optimized for infiltration by any particular material, they are potentially applicable as templates for 3D PhCs.

This work was supported in part by the Asian Office of Air Force Research and Development, contract F62562-03-P-0208 AORD 02-35. H. Misawa's e-mail address is misawa@es.hokudai.ac.jp.

References

1. E. Yablonovitch, Phys. Rev. Lett. **58,** 2059 (1987).
2. J. D. Joannopoulos, P. R. Villeneuve, and S. Fan, Nature **386,** 143 (1997).
3. S. Lin, J. Flemming, D. Hetherington, B. Smith, R. Biswas, K. Hot, M. Sigalas, W. Zubrycki, S. Kurtz, and J. Bur, Nature **394,** 251 (1998).
4. S. Noda, K. Tomoda, N. Yamamoto, and A. Chutinan, Science **289,** 604 (2000).
5. P. N. Pusley and W. van Megen, Nature **320,** 340 (1986).
6. H. Míguez, C. López, F. Meseguer, Á. Blanco, L. Vásquez, and R. Mayoral, Appl. Phys. Lett. **71,** 1148 (1996).
7. H. Míguez, A. Blanco, F. Meseguer, C. López, H. M. Yates, M. E. Pemble, V. Fornés, and A. Mifsud, Phys. Rev. B **59,** 1563 (1999).
8. A. Blanco, E. Chomski, S. Grabtchak, M. Ibisate, S. John, S. Leonard, C. Lopez, F. Meseguer, H. Miguez, J. Mondia, G. A. Ozin, O. Toader, and H. M. van Driel, Nature **405,** 437 (2000).
9. S. Kawata, H.-B. Sun, T. Tanaka, and K. Takada, Nature **412,** 697 (2001).
10. B. Cumpston, S. Ananthavel, S. Barlow, D. Dyer, J. Ehrlich, L. Erskine, A. Heikal, S. Kuebler, I.-Y. Lee, D. Mccord-Maughon, J. Qin, H. Röckel, M. Rumi, X.-L. Wu, S. R. Marder, and J. V. Perry, Nature **398,** 51 (1999).
11. H. Misawa, H. Sun, S. Juodkazis, M. Watanabe, and S. Matsuo, Proc. SPIE **3933,** 246 (2000).
12. H. Sun, S. Matsuo, and H. Misawa, Appl. Phys. Lett. **74,** 786 (1999).
13. H. Sun, V. Mizeikis, Y. Xu, S. Juodkazis, J.-Y. Ye, S. Matsuo, and H. Misawa, Appl. Phys. Lett. **79,** 1 (2001).
14. M. Straub and M. Gu, Opt. Lett. **27,** 1824 (2002).
15. Yu. V. Miklyaev, D. C. Meisel, A. Blanco, G. von Freymann, K. Busch, W. Koch, C. Enkrich, M. Deubel, and M. Wegener, Appl. Phys. Lett. **82,** 1284 (2003).
16. "SU-8 resists," (MicroChem Corp., Newton, Mass.), http://www.microchem.com/products/su_eight.htm.
17. K. M. Ho, C. Chan, C. Soukoulis, R. Biswas, and M. Sigalas, Solid State Commun. **89,** 413 (1994).
18. G. Witzgall, R. Vrijen, E. Yablonovitch, V. Doan, and B. Schwartz, Opt. Lett. **22,** 1745 (1998).
19. S. Noda, Physica B **279,** 142 (2000).
20. J. Pendry and A. MacKinnon, Phys. Rev. Lett. **69,** 2772 (1992).
21. J. D. Joannopoulos, R. D. Meade, and J. N. Winn, *Photonic Crystals: Molding the Flow of Light* (Princeton U. Press, Princeton, N.J., 1995).
22. M. Straub, M. Ventura, and M. Gu, Phys. Rev. Lett. **91,** 043901 (2003).